Journal of Translational Medicine

RESEARCH

Open Access

SLC38A5 suppresses ferroptosis through glutamine-mediated activation of the PI3K/AKT/mTOR signaling in osteosarcoma

Xinghan Huang[1†], Kezhou Xia[1†], Zhun Wei[1†], Wenda Liu[1], Zicheng Wei[1] and Weichun Guo[1*]

Abstract

Background Solute carrier family 38 member 5 (SLC38A5) is an amino acid transporter that plays a significant role in various cellular biological processes and may be involved in regulating the progression of tumors However, its function and underlying mechanism in osteosarcoma remain unexplored.

Methods Utilizing various database analyses and experiments, we have explored the dysregulation of SLC38A5 in osteosarcoma and its prognostic value. A series of in vitro functional experiments, including CCK-8, colony formation, wound healing, and transwell invasion assays, were conducted to evaluate the effects of SLC38A5 on the proliferation, migration, and invasion of osteosarcoma cells. Downstream pathways of SLC38A5 were explored through methods such as western blot and metabolic assays, followed by a series of validations. Finally, we constructed a subcutaneous xenograft tumor model in nude mice to explore SLC38A5 function in vivo.

Results SLC38A5 is upregulated in osteosarcoma and is associated with poor prognosis in patients. Upregulation of SLC38A5 promotes proliferation, migration, and invasion of osteosarcoma cells, while the PI3K inhibitor BKM120 can counteract these effects. Additionally, silencing of SLC38A5 inhibits tumor growth in vivo. Mechanistically, SLC38A5 mediates the activation of the PI3K/AKT/mTOR signaling pathway by transporting glutamine, which subsequently enhances the SREBP1/SCD-1 signaling pathway, thereby suppressing ferroptosis in osteosarcoma cells.

Conclusion SLC38A5 promotes osteosarcoma cell proliferation, migration, and invasion via the glutamine-mediated PI3K/AKT/mTOR signaling pathway and inhibits ferroptosis. Targeting SLC38A5 and the PI3K/AKT signaling axis may provide a meaningful therapeutic strategy for the future treatment of osteosarcoma.

†Xinghan Huang, Kezhou Xia and Zhun Wei authors have contributed equally to this work and share the first authorship.

*Correspondence:
Weichun Guo
guoweichun@aliyun.com

Full list of author information is available at the end of the article

Graphical abstracts

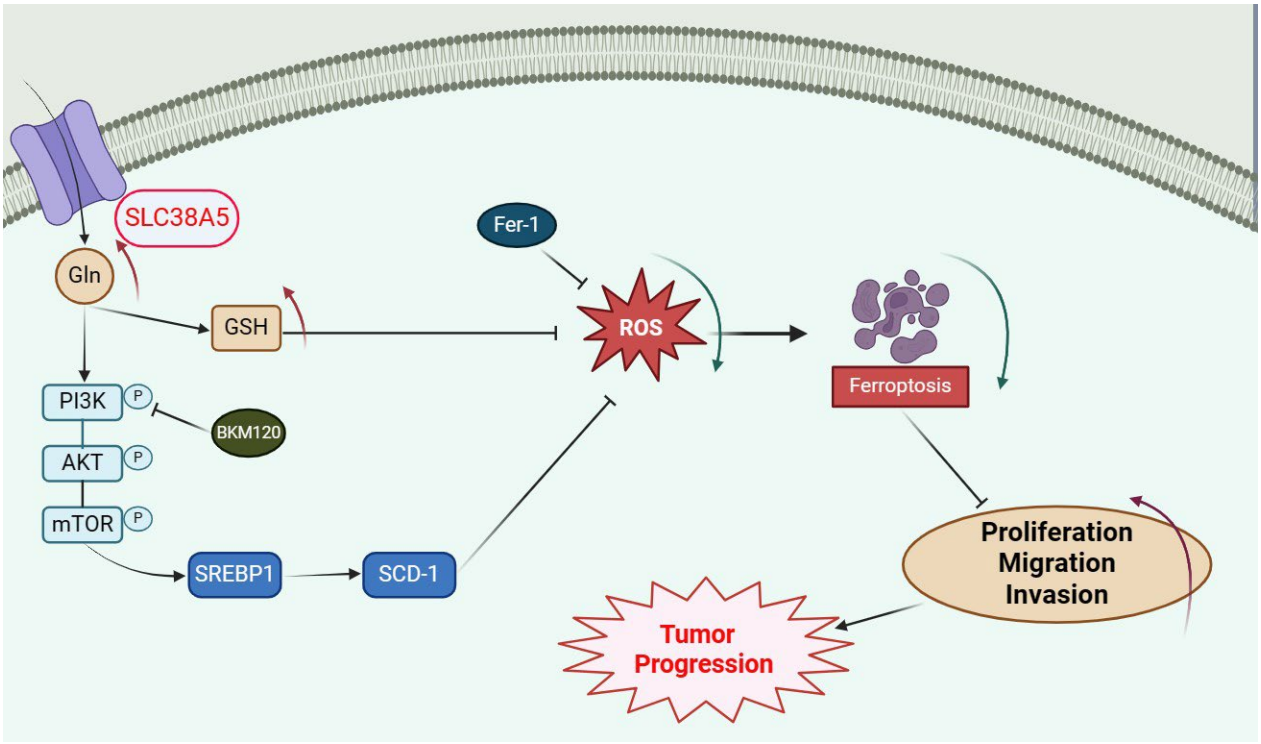

Keywords Osteosarcoma, SLC38A5, PI3K/AKT/mTOR pathway, glutamine, ferroptosis

Introduction

Osteosarcoma is a bone tumor that originates from the malignant proliferation of mesenchymal cells that produce bone-like stroma [1]. It is the most common primary bone malignant tumor, which occurs in adolescents or children with rapid bone growth and development. According to epidemiological statistics, the combined incidence of osteosarcoma is 1 ~ 3 cases annually per million [2]. Although rare, osteosarcoma is one of the leading causes of cancer-related deaths in adolescents [3]. Surgery combined with neoadjuvant chemotherapy (preoperative and postoperative chemotherapy; doxorubicin and cisplatin with or without methotrexate) is for now the standard of care for patients with osteosarcoma, which has greatly improved the prognosis for patients with primary osteosarcoma, with 5-year survival rates increasing to 70% [4]. Nevertheless, the prognosis remains poor for patients who relapse or suffer metastases, with 5-year survival rates still below 20% [5]. Therefore, exploring the specific mechanisms of osteosarcoma development and screening for new therapeutic targets are of great significance to the diagnosis and treatment of osteosarcoma.

Glutamine is the most abundant non-essential amino acid in the body and the most abundant circulating amino acid, which is a key carbon and nitrogen donor and energy source for the body [6]. It was shown that tumor cells take up large amounts of glutamine for their own biosynthesis, growth and proliferation, regulation of signaling pathways and maintenance of redox homeostasis; consequently, upregulation of glutamine transporter proteins on the cell membrane is required [7, 8]. Solute carrier (SLC) transporters are a family of more than 300 membrane-bound proteins that facilitate the transport of a wide range of substrates across biological membranes and play an essential role in cellular uptake of nutrients [9]. Solute carrier family 38 member 5 (SLC38A5), also known as sodium-coupled neutral amino acid transporter 5 (SNAT5), was functionally identified as the amino acid transport system N, which selectively transports amino acids such as glutamine, aspartic acid and histidine across cell membranes [10]. Moreover, since the function of system N transporters is associated with H flux with a significant impact on intracellular pH, the role of SLC38A5 for glutamine transport is more applicable to tumor cells [11]. Conjecturally, it may be advantageous for tumor cells to up-regulate SLC38A5. In recent years, more attention was paid to the functions of SLC38A5 in malignant tumors. For example, SLC38A5 was reported be a tumor promoter in pancreatic cancer, and its

overexpression leads to poor overall survival in patients with pancreatic cancer [12]. Furthermore, in breast cancer, upregulation of SLC38A5 induces cell proliferation by inducing micropinocytosis [13]. In another report, SLC38A5 promotes tumor growth by inhibiting cisplatin chemosensitivity in breast cancer cells [14]. These studies suggest that SLC38A5 may play an essential role in various tumors; however, the specific functional role of SLC38A5 in osteosarcoma and its underlying mechanism remain unclear.

In this study, we aimed to determine the role of SLC38A5 in osteosarcoma based on its importance as an amino acid transporter in tumors. To this end, we investigated the effects of SLC38A5 on osteosarcoma cells both in vitro and in vivo, and unveiled the molecular mechanism by which SLC38A5 regulates ferroptosis and influences the malignancy of osteosarcoma. SLC38A5 may serve as a prognostic factor as well as a potential therapeutic target in osteosarcoma.

Materials and methods

Bioinformatic analysis

The Tumor Immune Estimation Resource (TIMER) database (https://cistrome.shinyapps.io/timer/) was used to demonstrate the differential expression of SLC38A5 in different tumor tissues and the corresponding normal tissues. We downloaded osteosarcoma cases from the TARGET database (https://portal.gdc.cancer.gov/) and the GEO database (https://www.ncbi.nlm.nih.gov/geo/). We excluded patients who lacked follow-up information or had unknown survival status, ultimately including a total of 139 cases in the survival analysis, consisting of 86 cases from the TARGET database and 53 cases from the GSE21257 dataset.

Clinical samples

The 12 groups of human osteosarcoma tissues and the corresponding adjacent normal tissues used in this study were obtained from patients with a histopathological diagnosis of osteosarcoma undergoing surgery at Renmin Hospital of Wuhan University. All patients signed informed consent, and the collection and use of human samples were approved by the Ethics Committee of the Renmin Hospital of Wuhan University. The ethics submission and approval is in accordance with the Helsinki Declaration.

Cell culture and transfection

The human osteosarcoma cell lines HOS, Saos-2 and MG63 were purchased from Wuhan Servicebio Technology Co., Ltd. The human osteoblast cell line hFOB1.19 and osteosarcoma cell lines 143B and U2OS were obtained from the National Collection of Authenticated Cell Cultures (Shanghai, China). Cells were cultured in RPMI-1640 medium (#PM150110, Procell, Wuhan, China) supplemented with 10% FBS (#A5670701, Gibco, USA) and 1% penicillin/streptomycin (#G4003, Servicebio, Wuhan, China) and were propagated with 5% CO_2 at 37 °C. For transfection, we constructed SLC38A5 overexpression (LV-SLC38A5), SLC38A5 knockdown (shSLC38A5), and the control (LV-Control and shNC) using the lentivirus obtained from OBiO (Shanghai, China). The PI3K inhibitor (BKM120) was purchased from MedChemExpress (USA). The siRNAs of SREBP1 and SCD-1 were obtained from OBiO (Shanghai, China). The primers sequences were:

siSREBP1-1: CCCTGTGCTGACGGAAGCCAA; siSREBP1-2: GCCATCGACTACATTCGCTTT; siSCD-1-1: CCTACGACAAGAACATTCAAT; siSCD-1-2: AGTTTCTAAGGCTACTGTCTT.

RNA sequencing and qRT-PCR

Cells stably transfected with shSLC38A5 and shNC were collected for RNA isolation. The TRIzol® Reagent (Invitrogen, USA) was used to extract total RNA from the shNC and shSLC38A5 143B cells, following the manufacturer's protocol. RNA concentration and purity was measured using NanoDrop 2000 (Thermo Fisher Scientific, Wilmington, DE). RNA integrity was assessed using the RNA Nano 6000 Assay Kit of the Agilent Bioanalyzer 2100 system (Agilent Technologies, CA, USA). Then, the RNA was sent to the BGI (Shenzhen, China) for RNA-seq analysis. Sequencing libraries were generated using Hieff NGS Ultima Dual-mode mRNA Library Prep Kit for Illumina (Yeasen Biotechnology (Shanghai) Co., Ltd.) following manufacturer's recommendations and index codes were added to attribute sequences to each sample. Briefly, mRNA was purified from total RNA using poly-T oligo-attached magnetic beads. Subsequently, 2×50 bp pair-end RNA sequencing was performed on the BGISEQ-500 platform according to the manufacturer's protocol. For subsequent investigation, RNA-seq data in the FPKM format were used. Differential expression analysis of two conditions/groups was performed using the DESeq2. Genes with an adjusted P-value < 0.01 & $|\log_2(\text{fold change})| > 1$ found by DESeq2 were assigned as differentially expressed. The qRT-PCR was performed using SYBR® Premix Ex Taq™ (TaKaRa, Tokyo, Japan). The primers sequences were: SLC38A5, forward,5'-AACCTGAGTCTGAGTTGCGG-3'and reverse,5'-AGGGAGGGCTCCATTCATCT-3'; GAPDH, forward,5'-TGCAACCGGGAAGGAAATGA-3'and reverse,5'-GCATCACCCGGAGGAGAAAT-3'. The mRNA expression of GAPDH was used as an internal control.

Western blot

Cell lysates were prepared in RIPA buffer (#G2002, Servicebio, Wuhan, China) with protease and phosphatase

inhibitors. After quantification of protein concentration using a BCA kit (#G2026, Servicebio, Wuhan, China), proteins (10 μg) were separated by SDS-PAGE and transferred onto PVDF membranes. Then, membranes were blocked in TBST buffer containing 5% non-fat milk for 2 h and incubated with primary antibodies overnight at 4 °C. After washing with TBST, the secondary antibody was incubated at room temperature and the membrane was detected with ECL reagent (#BL520B, Biosharp, China). The antibodies against SLC38A5 (1:1000, #ab72717), GPX4 (1:3000, #ab125066), Nrf2 (1:2000, #ab137550), SREBP1 (1:1000, #ab313881), SCD-1 (1:10000, #ab39969) were purchased from Abcam (Cambridge, UK). Antibodies targeting GAPDH (1:100000, #A19056), E-cadherin (1:1000, #A3044), N-cadherin (1:1000, #A3045), Vimentin (1:50000, #A19607), p-PI3K (1:3000, #A22730), PI3K (1:10000, #A0265), AKT (1:1000, #A18120), p-AKT (1:1000, #AP1208), p-mTOR (1:1000, #AP0978), mTOR (1:2000, #A2445) were obtained from Abclonal (Wuhan, China).

CCK-8 and colony formation assay

The assay of cell proliferation ability in this study was performed by CCK-8 and colony formation assays. Briefly, 4×10^3 cells in 100 μl culture were added into each well of a 96-well plate and daily measurements performed from day 1 to 5. At each time point, 10 μl of CCK-8 reagent (#C0037, Beyotime, China) was added to each well. The OD450 (optical density) was detected with a microplate reader. For colony formation assay, 5×10^2 cells were added into each well of a 6-well plate and incubated for 2 weeks. After washed and fixed, the colonies were stained with 0.1% crystal violet, then, photographed and counted.

Cell migration and invasion assay

The wound healing assay was used to test cell migration ability. Cells were seeded in 6-well plates, and when the cell density was about 90%, a wound was made in the center of the well using a 100 μl pipette tip. Subsequently, the cells were cultured in serum-free medium for 36 h. The wound was observed using an inverted microscope (Olympus, Japan) and measured by ImageJ.

Transwell invasion assay was conducted using transwell chambers and Matrigel (Corning, USA)0.1×10^5 cells in 200 μl serum-free medium were added into the upper chamber precoated with Matrigel, and 600 μl medium containing 20% FBS was added into the lower chamber. After incubation for 48 h, invaded cells were stained with 0.1% crystal violet and observed by an inverted microscopy.

Immunohistochemistry (IHC)

Tumor xenografts were fixed (4% Paraformaldehyde for 12 h), paraffin-embedded, and sectioned according to the standard protocol. The sections were deparaffinized with xylene, hydrated with alcohol. Antigen retrieval was performed using Tris-EDTA antigen retrieval solution (Servicebio, Wuhan, China) through the heat-induced antigen retrieval method. Subsequently, endogenous peroxidase was inactivated, and the sections were blocked with BSA. Subsequently, the sections were incubated with primary antibodies, SLC38A5 (1:200, #ab72717, Abcam), p-mTOR (1:100, #ab109268, Abcam), GPX4 (1:100, #ab125066, Abcam), N-cadherin (1:150, #A3045, Abclonal). Then the sections were cleaned and incubated with secondary antibodies. The chromogenic detection was performed using a DAB kit (CST, USA). The sections were examined and imaged with a brightfield microscope (Olympus, Japan).

Glutamine and Malondialdehyde measurement

According to the manufacturer's protocol, glutamine, glutathione and MDA levels were determined by the glutamine assay kit (#MAK438, Merck, Germany), the GSH assay kit and the lipid oxidation (MDA) assay kit (#S0131S, Beyotime, China). Glutamine was purchased from the Servicebio (Wuhan, China).

OCR and ECAR measurement

Oxygen consumption rate (OCR) and extracellular acidification rate (ECAR) were conducted following the manufacturer's protocol (Seahorse XFe24 Analyzer, Agilent). Briefly, cells were seeded onto XF-24 plates at a density of 5×10^5 cells/well for 24 h Then, they were incubated in XF assay media for 1 h at 37 °C in a non-CO_2 incubator and stressed with sequential addition of 1μM oligomycin, 2μM carbonyl cyanide p-(trifluoromethoxy) phenylhydrazone, and a 0.5μM cocktail of rotenone/antimycin A.

Animal models

Four-week-old male athymic mice were purchased from the Shulaibao Biotechnology (Wuhan, China), and reared in the Animal Center of Renmin Hospital of Wuhan University. All animal experiments were performed following the protocol approved by the Animal Care and Use Committee of Renmin Hospital of Wuhan University. The mice were randomly divided into two groups and subcutaneously injected with shSLC38A5 and shNC 143B cells. The mice were observed every two days for changes in diet, spirit, activity status and weight, and were assessed for pain and distress. Tumor volume was measured every 5 days, and the tumor volume was calculated as $V=L\times W^2/2$, where L and W are the longest and shortest diameters (mm). Four weeks after injection, all mice were sacrificed, and the tumors were collected for further analysis.

Statistical analysis

GraphPad Prism 8.0 and SPSS 15.0 were used for statistical analysis. All results are presented as mean ± standard deviation (SD), and differences between the groups were analyzed by Student's *t*-test and one-way ANOVA. $P<0.05$ was considered statistically significant.

Results

SLC38A5 is up-regulated in osteosarcoma and associated with a poor prognosis

To explore whether SLC38A5 is associated with tumor development, we analyzed the differential expression of SLC38A5 in various tumor tissues and adjacent normal tissues using the TIMER database. It can be seen that SLC38A5 expression was substantially increased in many malignancies such as breast invasive carcinoma (BRCA), cholangiocarcinoma (CHOL), colon adenocarcinoma (COAD), head and neck squamous cell carcinoma (HNSC), liver hepatocellular carcinoma (LIHC), rectum adenocarcinoma (READ) and stomach adenocarcinoma (STAD), compared to the adjacent normal tissues. However, it was shown to be decreased in kidney chromophobe (KICH), lung adenocarcinoma (LUAD), prostate adenocarcinoma (PRAD) and uterine corpus endometrial carcinoma (UCEC) (Fig. 1A). Regarding osteosarcoma, our qRT-PCR and western blot results of osteosarcoma samples showed a notably increase in mRNA and protein level of SLC38A5 in osteosarcoma tissues compared to adjacent normal tissues (Fig. 1B-D). Meanwhile, we conducted verification at the cellular level. The SLC38A5 expression was significantly elevated in the osteosarcoma cell lines (HOS, Saos-2, MG63, U2OS, 143B) compared to human osteoblastic cell line (hFOB 1.19), both at the mRNA and protein level (Fig. 1E-G). Furthermore, we performed a Kaplan-Meier analysis to determine the prognostic value of SLC38A5 using data from the TARGET and GEO databases. The results showed that the survival rate of patients in the SLC38A5 high-expression group was significantly lower than that in the low-expression group (Fig. 1H-I).

SLC38A5 induces cell proliferation, migration and invasion in osteosarcoma

To investigate the role of SLC38A5 in osteosarcoma progression, we upregulated its expression in osteosarcoma cells by constructing recombinant lentivirus. The significantly upregulated expression of SLC38A5 in LV-SLC38A5 group cells was verified by qRT-PCR and western blot (Fig. 2A-C). Initially, we evaluated the proliferation ability of cells using CCK-8 and colony formation assay. It can be observed that the cellular viability and the number of colony in the LV-SLC38A5 group were conspicuously higher than those in the control group (Fig. 2D-G). These findings suggested that overexpression of SLC38A5 had a positive impact on the proliferation and clonogenic potential of osteosarcoma cells. Furthermore, the results of transwell invasion and wound healing assay demonstrated that cells with higher SLC38A5 expression possess stronger invasion and migration capabilities (Fig. 2H-L). We also assessed the expression of epithelial–mesenchymal transition (EMT)-related proteins. Remarkably, the western blot revealed a significant decrease of E-cadherin level, whereas the levels of N-cadherin and Vimentin increased (Fig. 2M-O). Collectively, our findings indicate that SLC38A5 stimulates the proliferation, migration and invasion capacity of osteosarcoma cells in vitro.

Silencing of SLC38A5 weakens cell proliferation, migration and invasion in osteosarcoma

Based on the aforementioned findings, we further delved into the potential impact of SLC38A5 knockdown on the malignant behavior of osteosarcoma cells. By utilizing lentivirus-mediated shSLC38A5 infection, we successfully established SLC38A5 knockdown cell lines. Subsequently, we validated the reduction of SLC38A5 expression through qRT-PCR and western blot analyses (Fig. 3A-C). The results from the CCK-8 and colony formation assay both demonstrated a significant decrease in cell number and colony formation, respectively, in the shSLC38A5 group compared to the control group (Fig. 3D-G). Similarly, the results of the transwell invasion and wound healing assay indicated that downregulation of SLC38A5 significantly impeded the invasion and migration of osteosarcoma cells (Fig. 3H-L). Furthermore, western blot results revealed a significant decrease in the protein levels of N-cadherin and Vimentin, whereas the expression level of E-cadherin was markedly increased (Fig. 3M-O). Overall, our results demonstrate that the absence of SLC38A5 significantly weakens the malignancy of osteosarcoma cells.

SLC38A5 promotes PI3K/AKT/mTOR signaling pathway in osteosarcoma

To delve deeper into the molecular mechanisms underlying SLC38A5's role in these malignant cellular behaviors, we performed RNA-seq analysis subsequent to SLC38A5 silencing in 143B cells. A total of 653 differentially expressed genes (DEGs) were identified, with 404 genes down-regulated and 249 genes up-regulated upon SLC38A5 knockdown (Fig. 4A-B). The subsequent KEGG enrichment analysis revealed that the DEGs were mainly concentrated within the PI3K/AKT signaling pathway (Fig. 4C). Given the significant role of the PI3K/AKT signaling pathway in cell proliferation, migration, and invasion, and its dysregulation being closely related to the malignant progression of osteosarcoma [15–17], we hypothesize that SLC38A5 is intimately associated with

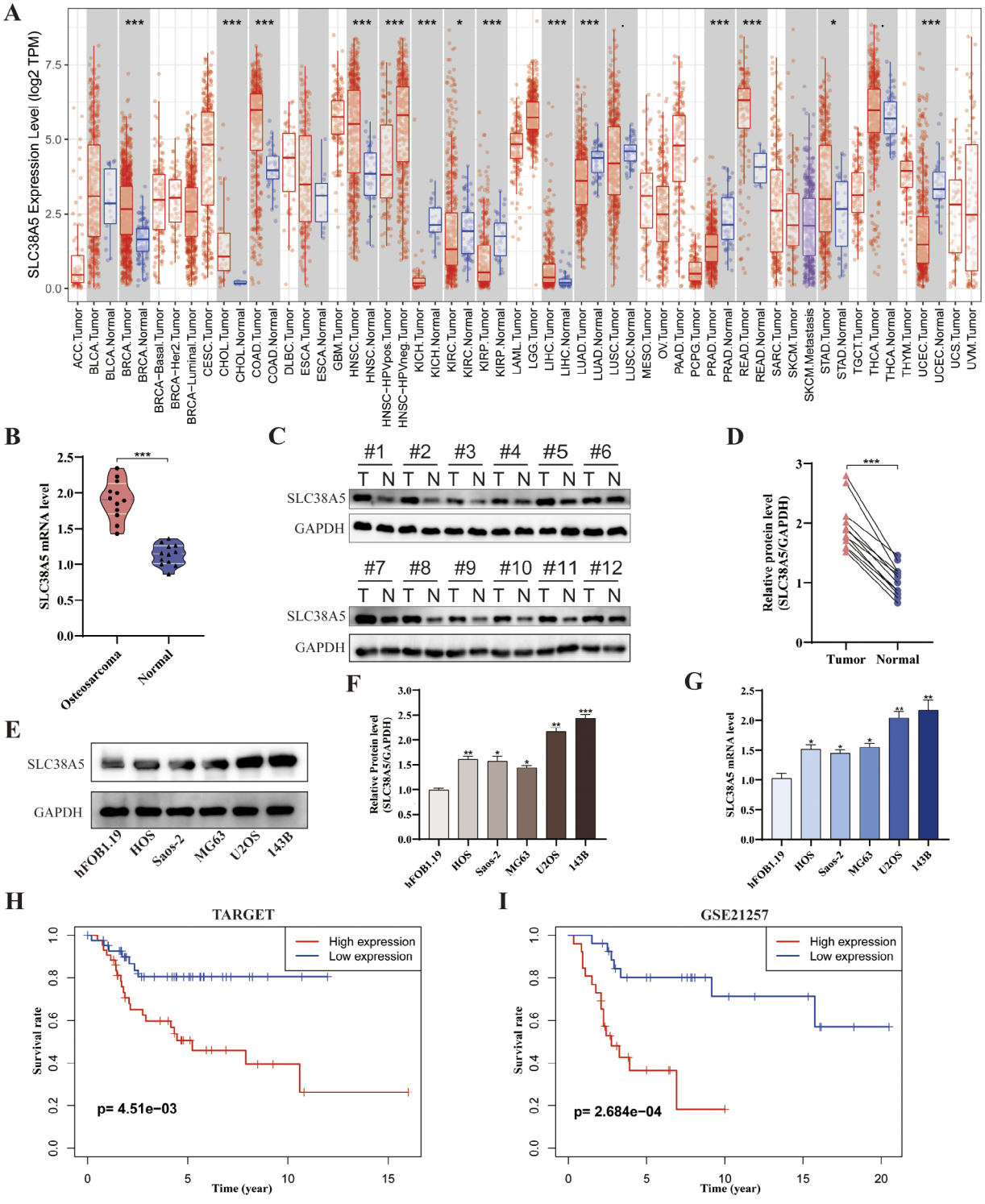

Fig. 1 SLC38A5 is up-regulated in osteosarcoma and associated with a poor prognosis. (**A**) The expression patterns of SLC38A5 across various tumors in the TCGA dataset based on the TIMER database. (**B**) The relative mRNA level of SLC38A5 in tumor ($n=12$) and adjacent normal tissues ($n=12$) based on clinical samples. (**C**) The protein level of SLC38A5 was assessed in osteosarcoma tissues and adjacent normal counterparts using western blot. (**D**) The quantitative analysis of the western blot result. (**E-F**) The protein level of SLC38A5 in human osteoblastic cell (hFOB1.19) and osteosarcoma cell lines (HOS, Saos-2, MG63, U2OS, 143B). (**G**) The mRNA level of SLC38A5 in different cell lines. (H-I) Kaplan–Meier survival analysis of SLC38A5 in osteosarcoma based on the TARGET database ($n=86$) and GSE21257 dataset ($n=53$). The median value of SLC38A5 expression is the cut-off for high and low expression. Results from three independent experiments are summarized in a histogram format. * $P<0.05$, ** $P<0.01$, *** $P<0.001$

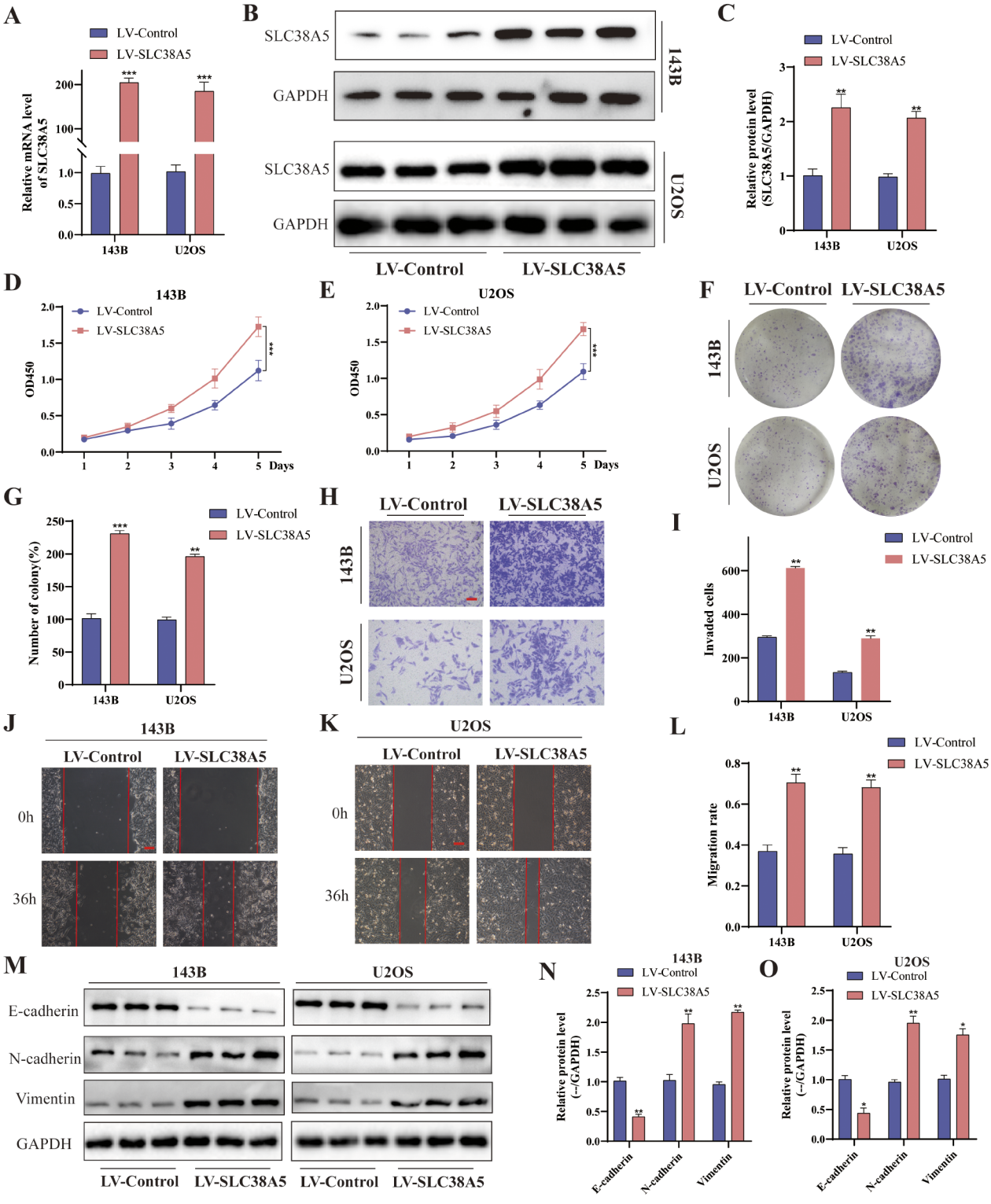

Fig. 2 Overexpression of SLC38A5 induces cell proliferation, migration and invasion in osteosarcoma. (**A**) The qRT-PCR analysis of SLC38A5 in 143B and U2OS cells after infection of SLC38A5 overexpression lentivirus. (**B-C**) Western blot showed SLC38A5 protein levels in LV-SLC38A5 and LV-Control groups cells. (**D-E**) CCK-8 assay was conducted to evaluate the proliferation capacity of the LV-SLC38A5 and LV-Control groups cells. (**F-G**) Colony formation assay was performed to measure the colony formation ability of the two groups of cells. (**H-I**) Increased expression of SLC38A5 increased cell invasion ability based on transwell invasion assay, scale bar: 400 μm.(**J-L**) Representative images and quantitative analysis of wound healing assay showed the cell migration ability, scale bar: 200 μm. (**M-O**) Western blot analysis of EMT-related proteins including E-cadherin, N-cadherin and Vimentin. Results from three independent experiments are summarized in a histogram format. * $P < 0.05$, ** $P < 0.01$, *** $P < 0.001$

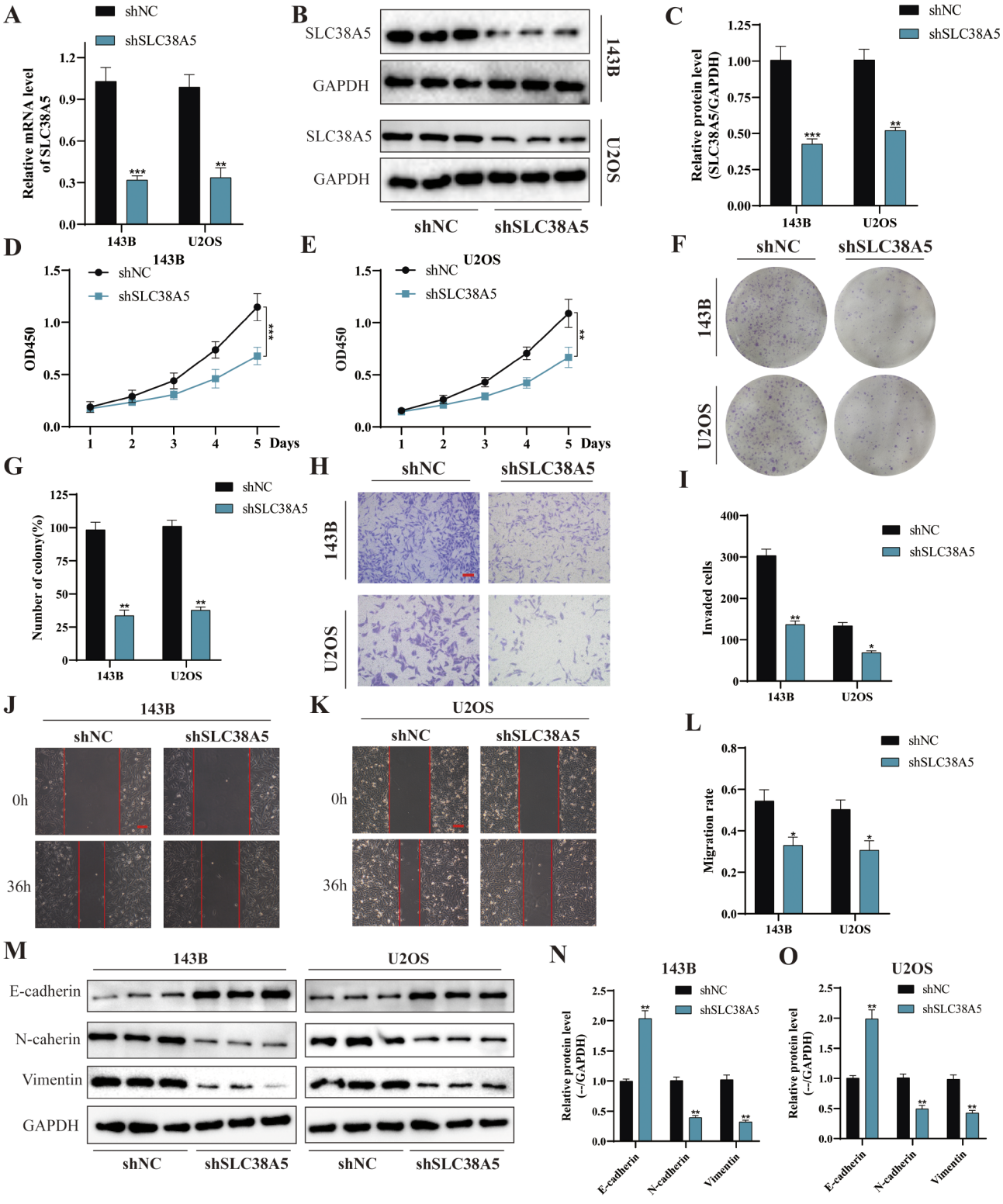

Fig. 3 Silencing of SLC38A5 weakens cell proliferation, migration and invasion in osteosarcoma. (**A-C**) The stable knockdown of SLC38A5 was validated through qRT-PCR and western blot. (**D-E**) CCK-8 assay showed the proliferation level of osteosarcoma cells in shSLC38A5 and shNC groups. (**F-G**) The knockdown of SLC38A5 significantly weakened colony formation ability of osteosarcoma cells. (**H-I**) Representative images and quantitative analysis of transwell invasion assay showed the cell invasion ability, scale bar: 400 μm. (**J-L**) The cell migration ability was determined using wound healing assay, scale bar: 200 μm. (**M-O**) Western blot analysis of EMT-related proteins including E-cadherin, N-cadherin and Vimentin. Results from three independent experiments are summarized in a histogram format. * $P<0.05$, ** $P<0.01$, *** $P<0.001$

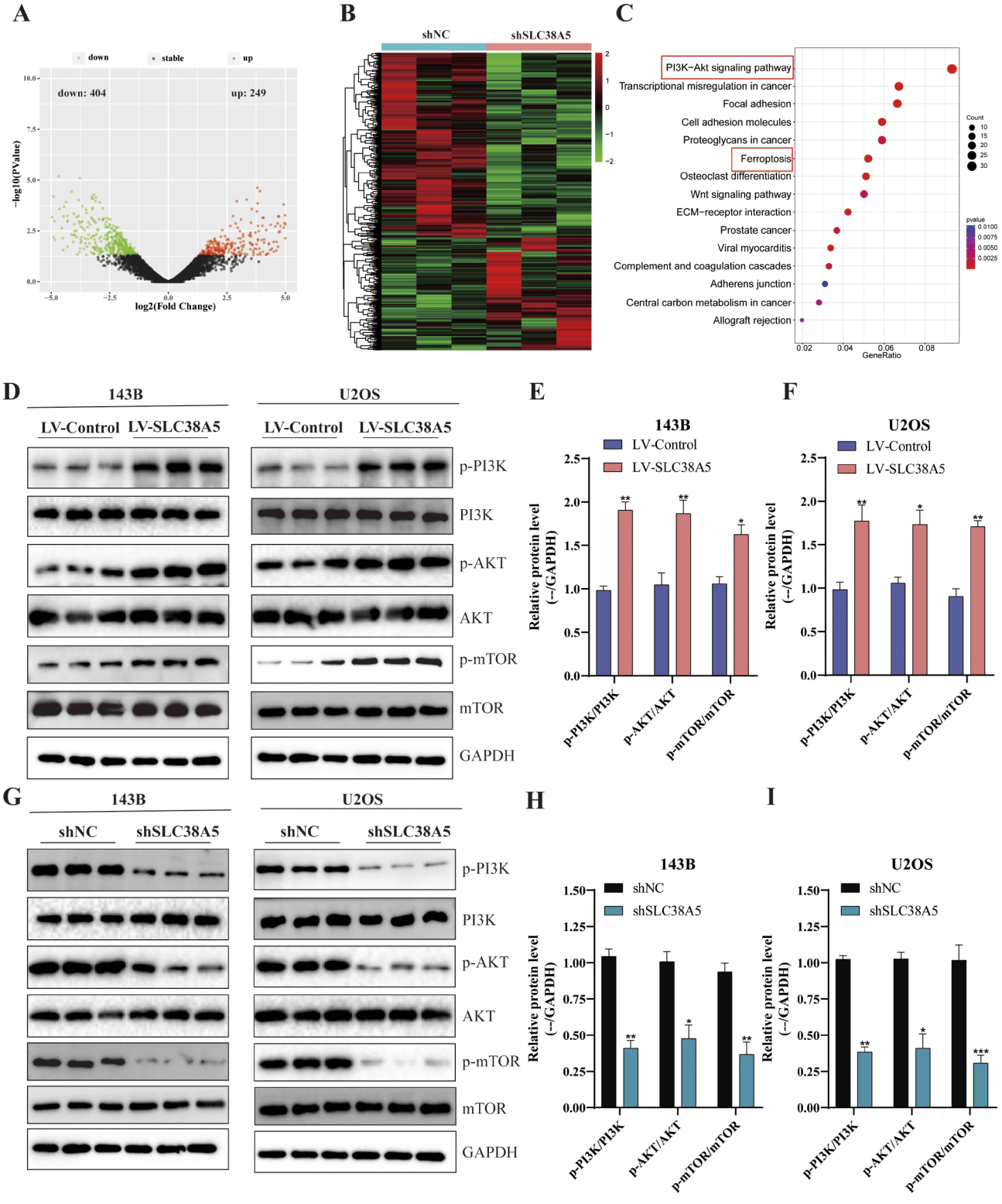

Fig. 4 SLC38A5 promotes PI3K/AKT/mTOR signaling pathway in osteosarcoma cells. (**A-B**) The differentially expressed genes between the shSLC38A5 and shNC groups were visualized through volcano plot and heatmap. DEGs were identified with a cutoff of | log2(fold change) | >1 and adjusted P-value < 0.05. (**C**) KEGG enrichment analysis of the DEGs. (**D-F**) The protein levels of p-PI3K, PI3K, p-AKT, AKT, p-mTOR and mTOR in osteosarcoma cells from the LV-SLC38A5 and LV-Control group using western blot. (**G-I**) The protein levels of p-PI3K, PI3K, p-AKT, AKT, p-mTOR and mTOR in osteosarcoma cells from the shSLC38A5 and shNC group using western blot. Results from three independent experiments are summarized in a histogram format. * $P < 0.05$, ** $P < 0.01$, *** $P < 0.001$

the PI3K/AKT signaling pathway. Thus, we investigated alterations in pivotal elements of the PI3K/AKT signaling pathway subsequent to the upregulation and downregulation of SLC38A5. The western blot results indicated that overexpression of SLC38A5 markedly enhanced the levels of p-PI3K, p-AKT and p-mTOR in osteosarcoma cells (Fig. 4D-F). Correspondingly, the expression of p-PI3K, p-AKT and p-mTOR was significantly reduced in osteosarcoma cells with SLC38A5 knockdown (Fig. 4G-I). The aforementioned results suggest that SLC38A5 promotes the PI3K/AKT/mTOR signaling pathway in osteosarcoma cells.

PI3K inhibitor can counteract the effect of SLC38A5 in promoting osteosarcoma progression

To confirm the modulatory effect of PI3K/AKT/mTOR signaling pathway on the malignancy of osteosarcoma cells induced by SLC38A5, we delved into the influence of the PI3K inhibitor BKM120 in this process. We added BKM120 to the culture medium of both the LV-SLC38A5 and LV-Control groups of osteosarcoma cells, and thereafter analyzed the modifications in their proliferation, migration, and invasion potentials. The CCK-8 and colony formation assay revealed that the upregulation of SLC38A5 markedly enhanced the proliferation capacity of osteosarcoma cells, whereas the inclusion of BKM120 mitigated this effect (Fig. 5A-C, E). The wound healing and transwell invasion assays yielded comparable findings, demonstrating that BKM120 can attenuate the stimulatory effect of SLC38A5 on the migration and invasion capabilities of osteosarcoma cells (Fig. 5D, F-I). Furthermore, we compared the relative change before and after the addition of BKM120 between the LV-Control and LV-SLC38A5 groups. The results indicated that cells with hyperactivated PI3K/AKT pathway were more sensitive to BKM120 than the control cells (Supplementary Fig. 1A-B). The results of western blot also indicated that BKM120 treatment attenuated the upregulation of N-cadherin, Vimentin, p-PI3K, p-AKT and p-mTOR as well as the downregulation of E-cadherin, which were induced by the overexpression of SLC38A5 (Fig. 5J-L, and Supplementary Fig. 1C-E). In conclusion, PI3K inhibitor can diminish the oncogenic effect of SLC38A5 and partially counteract the enhancement of malignant behaviors in osteosarcoma cells mediated by the upregulation of SLC38A5. This further underscores the pivotal role of the PI3K/AKT/mTOR signaling pathway in regulating the malignant behaviors of osteosarcoma cells.

SLC38A5 enhances glutamine uptake and inhibits ferroptosis in osteosarcoma

Due to the need for rapid proliferation and migration, cancer cells are more dependent on nutrients than normal cells, and glutamine serve as the primary fuel utilized by cancer cells. Since SLC38A5 acts as a transporter protein that can transport glutamine, we used the glutamine assay kit to investigate whether SLC38A5 modulates glutamine utilization in osteosarcoma cells. Our observations indicated that disruption of SLC38A5 expression led to a predictable decrease in glutamine uptake of osteosarcoma cells (both 143B and U2OS); conversely, when SLC38A5 expression was upregulated in osteosarcoma cells, the glutamine uptake rate also increased accordingly (Fig. 6A, and Supplementary Fig. 2A). Upon entering the cell, glutamine engages in multiple reactions within the mitochondria, which are intricately tied to mitochondrial function and play a pivotal role in various cellular activities. Consequently, we used the Seahorse XFe24 Analyzer to assess mitochondrial activity by quantifying the oxygen consumption rate (OCR) and extracellular acidification rate (ECAR) of the cells. The results demonstrated that cell mitochondrial function was inhibited in the shSLC38A5 group, with decreased levels of both OCR and ECAR (Fig. 6B-C). In contrast, they were elevated in the LV-SLC38A5 group, when compared to the control group (Supplementary Fig. 2B-C). Additionally, in our previous KEGG analysis, SLC38A5 displayed certain correlations with ferroptosis (Fig. 4C). Following this, we measured the levels of glutathione (GSH), malondialdehyde (MDA) and reactive oxygen species (ROS) within the cells. Our findings revealed that knockdown of SLC38A5 led to a depletion of GSH levels and an accumulation of MDA and ROS (Fig. 6D-E, and Supplementary Fig. 2D). Furthermore, western blot results also indicated that downregulation of SLC38A5 was accompanied by reduced levels of the crucial ferroptosis regulators Nrf2 and GPX4 (Fig. 6G-H, and Supplementary Fig. 2E-F). Importantly, these effects were partially mitigated by the ferroptosis inhibitor Fer-1. In conclusion, our results suggest that knockdown of SLC38A5 can induce ferroptosis in osteosarcoma cells.

SLC38A5 inhibits ferroptosis in osteosarcoma cells through the glutamine-mediated PI3K/AKT/mTOR/SREBP1/SCD-1 axis

Recently, several studies have confirmed the close relationship between mTOR signaling transduction and ferroptosis [18, 19]. Based on this, we postulate that SLC38A5 diminishes ferroptosis in osteosarcoma cells via the activation of the PI3K/AKT/mTOR pathway. Initially, we assessed MDA and ROS levels as indicators of cellular peroxidation. Upon administering PI3K inhibitor alone, we observed an elevation in both MDA and ROS levels. However, when SLC38A5 was upregulated independently, there was a notable decrease in intracellular MDA and ROS levels. Additionally, we discovered that the presence of PI3K inhibitor significantly diminished the suppressive effect of SLC38A5 on MDA and

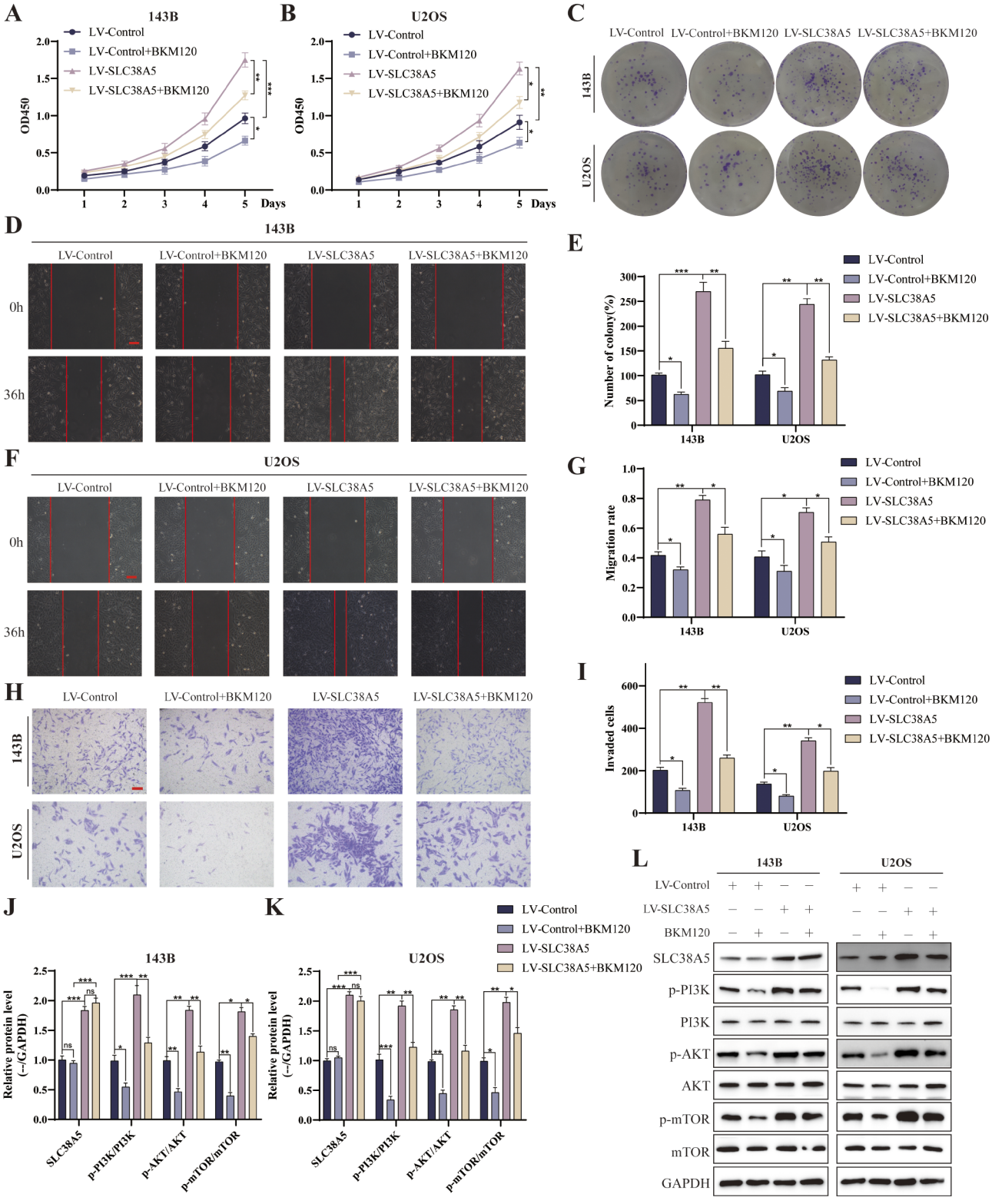

Fig. 5 PI3K inhibitor can counteract the effect of SLC38A5 in promoting osteosarcoma progression. (**A-B**) CCK-8 assay showed the proliferation level of osteosarcoma cells in the four groups. (**C**) Colony formation assay was performed to measure the colony formation ability of the four groups cells. (**D**) Representative images of wound healing assay showed the 143B cells migration ability, scale bar: 200 μm. (**E**) The quantitative analysis of colony formation assay. (**F-G**) Representative images and quantitative analysis of cell migration based on wound healing assay, scale bar: 200 μm. (**H-I**) The number of invasive cells in the four groups determined using transwell invasion assay. (**J-L**) Western blot was used to evaluate p-PI3K, PI3K, p-AKT, AKT, p-mTOR and mTOR in the four groups. Results from three independent experiments are summarized in a histogram format. * $P<0.05$, ** $P<0.01$, *** $P<0.001$, ns, not significant

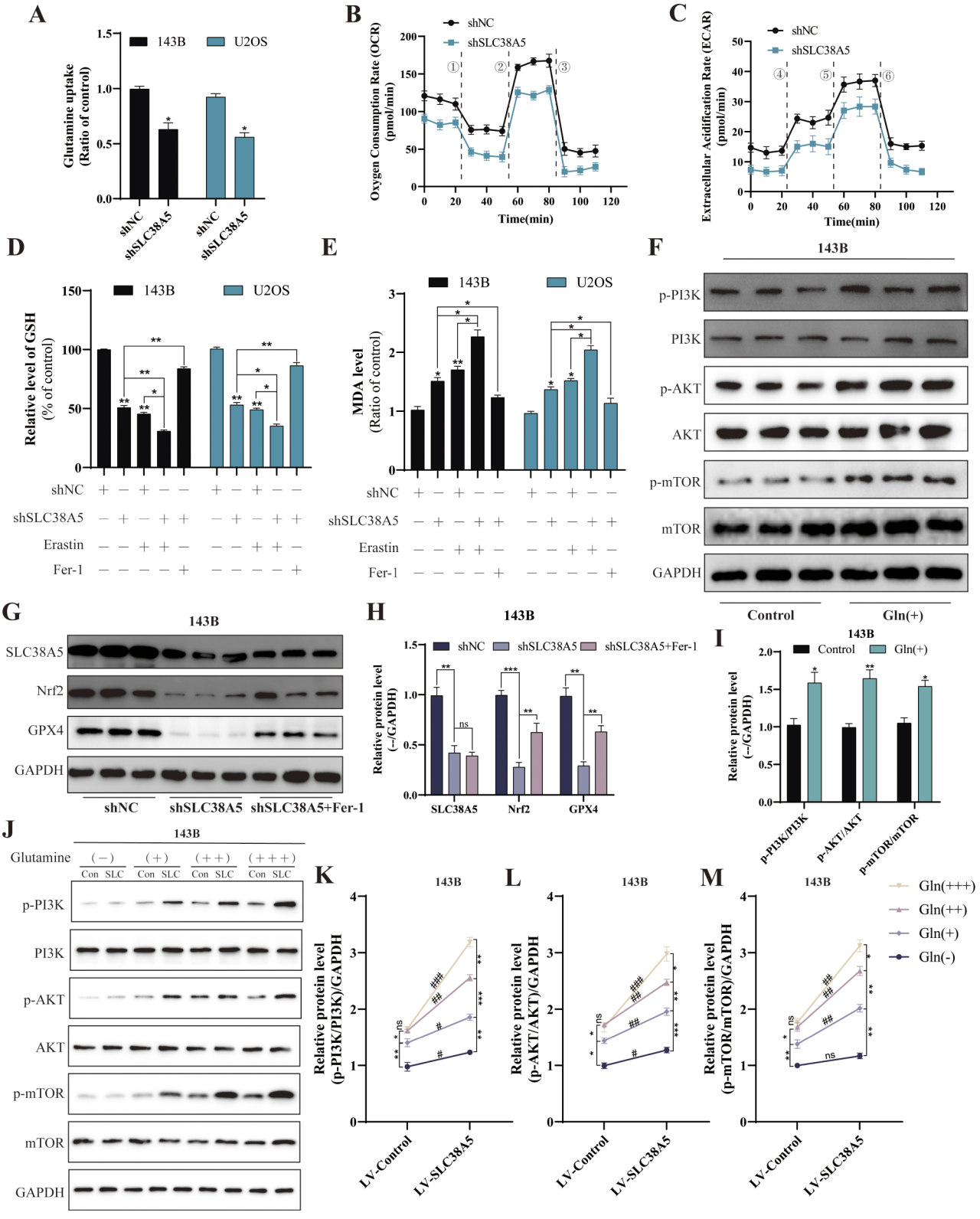

Fig. 6 (See legend on next page.)

(See figure on previous page.)

Fig. 6 SLC38A5 enhances glutamine uptake and inhibits ferroptosis in osteosarcoma cells. (**A**) Comparison of glutamine uptake of the shSLC38A5 and shNC groups cells. (**B-C**) The OCR and ECAR of 143B cells in the shSLC38A5 and shNC groups were measured and quantified, ① oligomycin, ② FCCP, ③ Rotenone & Antimycin A, ④ glucose, ⑤ oligomycin, ⑥ 2-DG. (**D-E**) The effect of SLC38A5 knockdown on GSH and MDA levels in osteosarcoma cells. (**F-I**) The 143B cells were treated with glutamine (2 mM) and incubated for 48 h, and then the key proteins of the PI3K/AKT/mTOR signaling pathway were detected by western blot. (**G-H**) Western blot analysis of ferroptosis-related proteins including Nrf2 and GPX4. (**J-M**) Under treatment with varying concentrations of glutamine, western blot was performed to detect the protein levels of p-PI3K, PI3K, p-AKT, AKT, p-mTOR, and mTOR in two groups of 143B cells. Con: LV-Control group; SLC: LV-SLC38A5 group. The concentrations were as follows: Gln(-): 0 mM, Gln(+): 2 mM, Gln(++): 5 mM, and Gln(+++): 10 mM. Results from three independent experiments are summarized in a histogram format. Comparison between different concentrations: * $P < 0.05$, ** $P < 0.01$, *** $P < 0.001$, ns, not significant. Comparison between different groups: # $P < 0.05$, ## $P < 0.01$, ### $P < 0.001$, ns, not significant

ROS levels (Fig. 7A-B). Interestingly, we found that the glutamine can also promote the activation of PI3K/AKT/mTOR pathway (Fig. 6F, I, and Supplementary Fig. 3A-B). Therefore, we further investigated the activation of the PI3K/AKT/mTOR signaling pathway in osteosarcoma cells under conditions of no, low, medium, and high concentrations of glutamine. Our Western blot results showed that in the absence of glutamine, SLC38A5 could promote the activation of the PI3K signaling pathway, but to a very low extent. Subsequently, within a certain range, as the concentration of glutamine increases, the activation of the PI3K/AKT/mTOR signaling pathway in the cells enhances. However, in the control group, when the glutamine concentration reaches 10mM, there is no further increase in the activation of the PI3K signaling pathway compared to 5mM. In contrast, in the SLC38A5 overexpression group, there is still a certain degree of enhancement (Fig. 6J-M, and Supplementary Fig. 3C-F). These results indicate that SLC38A5 inhibits ferroptosis in osteosarcoma cells via the glutamine-mediated activation of the PI3K/AKT/mTOR pathway. Chen et al. reported that in lung cancer, G protein-coupled estrogen receptor activates PI3K/AKT/mTOR signaling, inhibiting ferroptosis through SREBP1/SCD-1-mediated lipogenesis [19]. Thus, we delved into the potential role of this signaling pathway in mediating the SLC38A5-induced inhibition of ferroptosis in osteosarcoma cells. In line with our expectations, the upregulation of SLC38A5 prominently elevated the protein levels of SREBP1 and SCD-1 (Fig. 7C-D), which were partially mitigated by the administration of the PI3K inhibitor (Fig. 7E-F). Following that, we effectively silenced SREBP1 and SCD-1 in osteosarcoma cells using siRNA transfection and examined the subsequent effects on ferroptosis (Fig. 7G-J). We observed that knockdown of SREBP1 significantly increased MDA levels in osteosarcoma cells, but had little effect on ROS levels. In contrast, knockdown of SCD-1 led to an upregulation of both MDA and ROS levels. Furthermore, the knockdown of SREBP1 and SCD-1 significantly counteracted the inhibitory effect of SLC38A5 upregulation on MDA and ROS levels in osteosarcoma cells (Fig. 7K-L). In conclusion, our results demonstrate that SLC38A5 inhibits ferroptosis in osteosarcoma cells by enhancing the SREBP1/SCD-1 signaling pathway through the glutamine-mediated activation of the PI3K/AKT/mTOR signaling pathway.

SLC38A5 regulates tumor growth in vivo by mediating PI3K/AKT/mTOR signaling pathway and ferroptosis

To delve deeper into the functions of SLC38A5 in vivo, we employed shSLC38A5 and shNC 143B cells to construct a subcutaneous xenograft model in BALB/c nude mice. After the inoculation, the diameters of the tumors were measured every five days, and the growth trends were displayed in the form of curves. Based on the tumor growth curves, shSLC38A5 group exhibited slower tumor growth, accompanied by notable reductions in tumor size and weight, when compared to the shNC group (Fig. 8A-C). Subsequently, to further validate the influence of SLC38A5 on PI3K/AKT/mTOR signaling as well as on ferroptosis and EMT-associated proteins, we conducted detection via western blot. As depicted in Fig. 8D-G, compared to the shNC group, the expression levels of p-PI3K, p-AKT, p-mTOR, N-cadherin, Vimentin, Nrf2 and GPX4 were significantly reduced in the shSLC38A5 group, while the level of E-cadherin was markedly increased. In summary, these results further demonstrate that SLC38A5 promotes tumor growth in vivo through PI3K/AKT/mTOR signaling pathway and ferroptosis.

Discussion

Osteosarcoma is the most prevalent primary malignant bone tumor in adolescents, with extremely high malignancy. Despite extensive research, the etiology of osteosarcoma remains elusive in most cases, and the pursuit of common molecular therapeutic targets has been discouraging [4, 20]. Consequently, a profound investigation into the specific mechanisms underlying the initiation and progression of osteosarcoma is imperative.

An accumulating amount of evidence underscores the pivotal role of SLC transporters in numerous physiological functions, and that their malfunction disturbs the intracellular levels of various molecules and has been linked to the advancement of cancer [21, 22]. Although the function of SLC38A5 in many tumors are less well understood compared to other SLCs, as a system N transporter, the role of SLC38A5 in glutamine transport may be more applicable to tumor cells [11, 23]. However,

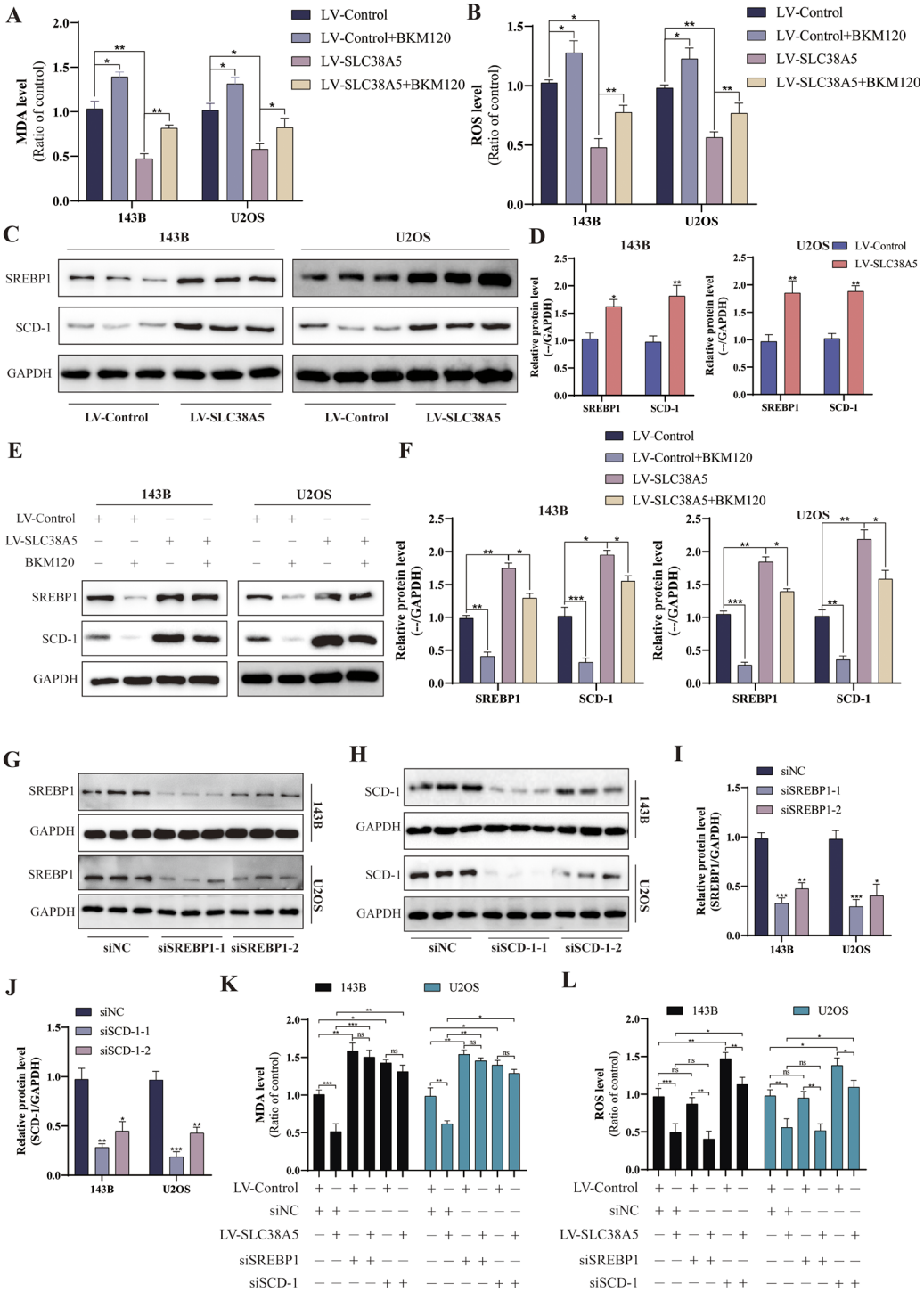

Fig. 7 SLC38A5 inhibits ferroptosis in osteosarcoma cells through the glutamine-mediated PI3K/AKT/mTOR/SREBP1/SCD-1 axis. (**A**) The MDA level of the osteosarcoma cells in the four groups. (**B**) The ROS level of the osteosarcoma cells in the four groups. (**C-D**) The protein levels of SREBP1 and SCD-1 in osteosarcoma cells from the the LV-SLC38A5 and LV-Control group using western blot. (**E-F**) Western blot was used to evaluate SREBP1 and SCD-1 in the four groups. (**G-J**) Western blot was used to validate the knockdown efficiency of SREBP1 and SCD-1 via siRNA transfection. **K-L**) The MDA and ROS levels of each group, compared with the control group. Results from three independent experiments are summarized in a histogram format. * $P < 0.05$, ** $P < 0.01$, *** $P < 0.001$

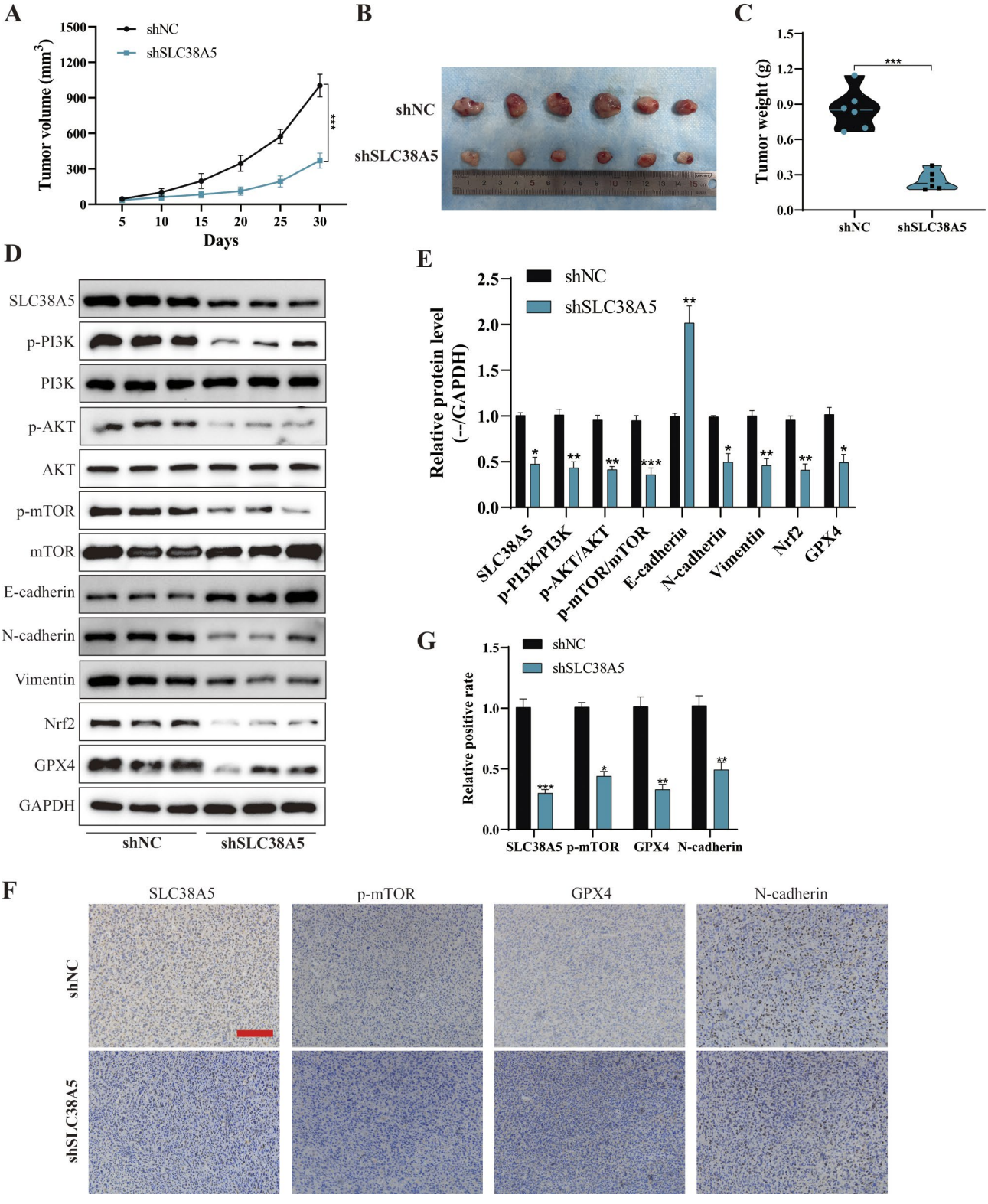

Fig. 8 SLC38A5 regulates tumor growth in vivo by mediating PI3K/AKT/mTOR signaling pathway and ferroptosis. (**A**) The growth curves of subcutaneous tumors in the shSLC38A5 and shNC groups. (**B**) Comparison of tumors obtained from nude mice of the two groups. (**C**) Tumor weight was compared between the two groups. (**D-E** Western blot and quantitative analyses of SLC38A5, p-PI3K, PI3K, p-AKT, AKT, p-mTOR, mTOR, E-cadherin, N-cadherin, Vimentin, Nrf2 and GPX4 in tumors. (**F-G**) IHC analysis of SLC38A5, p-mTOR, GPX4, N-cadherin for tissues of tumors, scale bar: 200 μm. Results from three independent experiments are summarized in a histogram format. * $P < 0.05$, ** $P < 0.01$, *** $P < 0.001$

its role and mechanism in osteosarcoma have not been elucidated until now. Our finding indicates that SLC38A5 acts an oncogenic role in osteosarcoma. Alternatively, we systematically analyzed the differences in SLC38A5 expression using human osteosarcoma tissue samples and cells, confirming the increased SLC38A5 expression in osteosarcoma tissues and cells. Additionally, among individuals diagnosed with osteosarcoma clinically, those with higher levels of SLC38A5 tend to have a worse prognosis compared to those with lower levels. Accordingly, SLC38A5 may serve as an independent risk factor for osteosarcoma. Furthermore, the upregulation of SLC38A5 prominently accelerated the proliferation, migration and invasion of osteosarcoma cells. Conversely, when SLC38A5 was knocked down, the malignancy of osteosarcoma was suppressed, leading to a slower growth rate in vivo. Overall, our work suggests that SLC38A5 is an oncogene and a potential prognostic factor for osteosarcoma, with the potential to emerge as a promising therapeutic target for the treatment of osteosarcoma.

To further elucidate the mechanisms underlying how SLC38A5 promotes cell proliferation, migration and invasion in osteosarcoma, we performed RNA-seq analysis that differentially expressed genes induced by SLC38A5 knockdown were mainly enriched in the PI3K/AKT signaling pathway and ferroptosis.

The PI3K/AKT/mTOR signaling pathway is one of the key signaling pathways in various types of cancers, playing a pivotal role in multiple cellular behaviors, including cell survival, proliferation, metastasis, and metabolism [24, 25]. Currently, abnormalities in the PI3K/AKT/mTOR signaling pathway have been widely implicated in the promotion of cancerous malignancy and progression [15]. In gastric cancer, APOC2 modulates the EMT process via the PI3K/AKT/mTOR signaling pathway, thereby facilitating GC progression and peritoneal metastasis [26]. Abnormal activation of PI3K/AKT/mTOR is also associated with breast cancer progression and the emergence of resistance to hormonal treatments [27]. The PI3K/AKT signaling pathway is also active in osteosarcoma. For instance, Li et al. showed that ZIP10 enhances the proliferation and chemoresistance of osteosarcoma cells through the stimulation of the PI3K/AKT pathway by ITGA10 [28]. To determine the function of SLC38A5 in modulating PI3K/AKT/mTOR signaling, we assessed the phosphorylation status of PI3K and AKT and mTOR following changes in SLC38A5 expression. Our findings suggest that SLC38A5 acts as a positive regulator of PI3K/AKT/mTOR signal activation. Furthermore, we found that BKM120, a PI3K inhibitor, can partially reverse the SLC38A5-mediated promotion of osteosarcoma cell proliferation, migration, and invasion. Therefore, we propose that the promotional effects of SLC38A5 on osteosarcoma are at least partially mediated through the PI3K/AKT/mTOR signaling pathway.

Cancer cells have traditionally been known to exhibit a pronounced dependence on glutamine metabolism as a defining trait [29–31]. According to a prior study, once glutamine enters the cell, it undergoes conversion to glutamate by glutaminase within the mitochondria, which then participates in the biosynthesis of GSH [32, 33]. GSH is an important antioxidant that can prevent oxidative stress and maintain the redox homeostasis in cells [34]. The redox state within cells is maintained in a dynamic equilibrium, and a lack of GSH can disrupt this balance, leading to the accumulation of ROS and ultimately causing cellular dysfunction and death [35, 36]. For cancer cells, high levels of oxidative stress make them more sensitive to GSH deficiency, thus reducing intracellular GSH levels is beneficial for many cancer treatment strategies [37]. Our findings revealed that in osteosarcoma cells with downregulated SLC38A5, there was a reduction in both glutamine uptake and GSH levels. This suggests that glutamine transported by SLC38A5 facilitates GSH synthesis in osteosarcoma cells. Consistent with this, we observed an increase in intracellular MDA and ROS levels when SLC38A5 was silenced.

Ferroptosis is a type of programmed cell death characterized by the accumulation of intracellular ROS [38]. In this study, we used the ferroptosis inhibitor Fer-1 to confirm the role of SLC38A5 in ferroptosis of osteosarcoma cells. Upon downregulation of SLC38A5, we observed a decline in intracellular GSH levels, accompanied by an elevation in MDA and ROS levels. However, as hypothesized, the introduction of Fer-1 partially reversed these alterations. Based on these results, we conclude that SLC38A5 inhibits ferroptosis in osteosarcoma cells. Interestingly, we also found that the increase of glutamine can also promote the activation of PI3K/AKT/mTOR pathway. Glutamine plays a pivotal role in the PI3K/AKT/mTOR signaling pathway promoted by SLC38A5. Moreover, we found that the PI3K inhibitor BKM120 can effectively reverse the inhibitory effect of SLC38A5 on ferroptosis. Therefore, we further explored the relationship between the PI3K/AKT/mTOR signaling pathway and ferroptosis. Chen et al. found that G protein-coupled estrogen receptor activates PI3K/AKT/mTOR signaling, inhibiting ferroptosis through SREBP1/SCD-1-mediated lipogenesis [19]. Another report also confirmed the close relationship between mTOR and SREBP1/SCD-1 with ferroptosis [39]. We hypothesize that similar associations may exist in osteosarcoma as well. Subsequently, we have designed siRNAs to interfere with the expression of SREBP1 and SCD-1. As anticipated, the knockdown of SREBP1 and SCD-1 significantly counteracted the inhibitory effect of SLC38A5 upregulation on MDA and ROS levels in osteosarcoma

cells. These results indicate that SLC38A5 inhibits ferroptosis in osteosarcoma cells by enhancing the SREBP1/SCD-1 signaling pathway through the glutamine-mediated activation of the PI3K/AKT/mTOR signaling pathway. Thus, our work indicates that SLC38A5 promotes osteosarcoma cell proliferation, migration and invasion via the glutamine-mediated PI3K/AKT/mTOR signaling pathway and inhibits ferroptosis.

Conclusions

Our work has elucidated the tumor-promoting role of SLC38A5 in osteosarcoma. Upregulation of SLC38A5 expression is often associated with a poor prognosis in osteosarcoma. Functionally, SLC38A5 promotes osteosarcoma cell proliferation, migration and invasion via the glutamine-mediated PI3K/AKT/mTOR signaling pathway and inhibits ferroptosis. Considering the intimate link between the aberrant activation of PI3K/AKT/mTOR signaling and the advancement of malignancies, as well as the reduction in GSH levels resulting from SLC38A5 inhibition, targeting SLC38A5 and the PI3K/AKT/mTOR holds promise in conferring multiple advantages, including enhancement of tumor therapeutic efficacy, inhibition of tumor cell proliferation and invasion. The integration of relevant targeted inhibitors with anticancer therapeutics presents a novel therapeutic strategy for osteosarcoma, offering potential to enhance the prognosis for the majority of patients with osteosarcoma.

Supplementary Information

The online version contains supplementary material available at https://doi.org/10.1186/s12967-024-05803-6.

Supplementary Material 1

Acknowledgements
We sincerely thank all those who devote much time to reading this thesis and give us much advice.

Author contributions
XH and WG designed the study; XH, KX, ZW and WL performed the experiments; KX and ZW analyzed the data; XH wrote the manuscript; All authors reviewed the manuscript.

Funding
This study was supported by funds from The Open Project of Hubei Key Laboratory (2023KFZZ022).

Data availability
The datasets used and/or analysed during the current study are available from the corresponding author on reasonable request.

Declarations

Ethics approval and consent to participate
All the experiments in our study were approved by the Ethics Committee of the Renmin Hospital of Wuhan University.

Consent for publication
All authors agreed to publish this study.

Competing interests
The authors declare that they have no known competing financial interests or personal relationships that could have appeared to influence the work reported in this paper.

Author details
[1]Department of Orthopaedics, Renmin Hospital of Wuhan University, 238 Jiefang Road, Wuhan 430060, China

Received: 23 August 2024 / Accepted: 24 October 2024
Published online: 07 November 2024

References

1. Kansara M, Teng MW, Smyth MJ, Thomas DM. <ArticleTitle Language="En">Translational biology of osteosarcoma. Nat Rev Cancer. 2014;14(11):722–35. https://doi.org/10.1038/nrc3838.
2. Mirabello L, Troisi RJ, Savage SA. International osteosarcoma incidence patterns in children and adolescents, middle ages and elderly persons. Int J Cancer. 2009;125(1):229–34. https://doi.org/10.1002/ijc.24320.
3. Ottaviani G, Jaffe N. The epidemiology of osteosarcoma. Cancer Treat Res. 2009;152:3–13. https://doi.org/10.1007/978-1-4419-0284-9_1.
4. Meltzer PS, Helman LJ. New Horizons in the Treatment of Osteosarcoma. N Engl J Med. 2021;385(22):2066–76. https://doi.org/10.1056/NEJMra2103423.
5. Gill J, Gorlick R. Advancing therapy for osteosarcoma. Nat Rev Clin Oncol. 2021;18(10):609–24. https://doi.org/10.1038/s41571-021-00519-8.
6. Stine ZE, Schug ZT, Salvino JM, Dang CV. Targeting cancer metabolism in the era of precision oncology. Nat Rev Drug Discov. 2022;21(2):141–62. https://doi.org/10.1038/s41573-021-00339-6.
7. Ma G, Zhang Z, Li P, Zhang Z, Zeng M, Liang Z, Li D, Wang L, Chen Y, Liang Y, Niu H. Reprogramming of glutamine metabolism and its impact on immune response in the tumor microenvironment. Cell Commun Signal. 2022;20(1):114. https://doi.org/10.1186/s12964-022-00909-0.
8. Jin J, Byun JK, Choi YK, Park KG. Targeting glutamine metabolism as a therapeutic strategy for cancer. Exp Mol Med. 2023;55(4):706–15. https://doi.org/10.1038/s12276-023-00971-9.
9. Lin L, Yee SW, Kim RB, Giacomini KM. SLC transporters as therapeutic targets: emerging opportunities. Nat Rev Drug Discov. 2015;14(8):543–60. https://doi.org/10.1038/nrd4626.
10. Mackenzie B, Erickson JD. Sodium-coupled neutral amino acid (System N/A) transporters of the SLC38 gene family. Pflugers Arch. 2004;447(5):784–95. https://doi.org/10.1007/s00424-003-1117-9.
11. Bhutia YD, Ganapathy V. Glutamine transporters in mammalian cells and their functions in physiology and cancer. Biochim Biophys Acta. 2016;1863(10):2531–9. https://doi.org/10.1016/j.bbamcr.2015.12.017.
12. Sniegowski T, Rajasekaran D, Sennoune SR, Sunitha S, Chen F, Fokar M, Kshirsagar S, Reddy PH, Korac K, Mahmud Syed M, Sharker T, Ganapathy V, Bhutia YD. Amino acid transporter SLC38A5 is a tumor promoter and a novel therapeutic target for pancreatic cancer. Sci Rep. 2023;13(1):16863. https://doi.org/10.1038/s41598-023-43983-1.
13. Ramachandran S, S RS, Sharma M, Thangaraju M, V VS, Sneigowski T, Y DB, Pruitt K, Ganapathy V. Expression and function of SLC38A5, an amino acid-coupled Na+/H + exchanger, in triple-negative breast cancer and its relevance to macropinocytosis. Biochem J. 2021;478(21):3957–76. https://doi.org/10.1042/BCJ20210585.
14. Shen X, Wang G, He H, Shang P, Yan B, Wang X, Shen W. SLC38A5 promotes glutamine metabolism and inhibits cisplatin chemosensitivity in breast cancer. Breast Cancer. 2024;31(1):96–104. https://doi.org/10.1007/s12282-023-01516-8.
15. Glaviano A, Foo ASC, Lam HY, Yap KCH, Jacot W, Jones RH, Eng H, Nair MG, Makvandi P, Geoerger B, Kulke MH, Baird RD, Prabhu JS, Carbone D, Pecoraro C, Teh DBL, Sethi G, Cavalieri V, Lin KH, Javidi-Sharifi NR, Toska E, Davids MS, Brown JR, Diana P, Stebbing J, Fruman DA, Kumar AP. PI3K/AKT/mTOR signaling transduction pathway and targeted therapies in cancer. Mol Cancer. 2023;22(1):138. https://doi.org/10.1186/s12943-023-01827-6.
16. Czarnecka AM, Synoradzki K, Firlej W, Bartnik E, Sobczuk P, Fiedorowicz M, Grieb P, Rutkowski P. Mol Biology Osteosarcoma Cancers (Basel). 2020;12(8). https://doi.org/10.3390/cancers12082130.
17. Zhang J, Yu XH, Yan YG, Wang C, Wang WJ. PI3K/Akt signaling in osteosarcoma. Clin Chim Acta. 2015;444:182–92. https://doi.org/10.1016/j.cca.2014.12.041.

18. Chen H, Qi Q, Wu N, Wang Y, Feng Q, Jin R, Jiang L. Aspirin promotes RSL3-induced ferroptosis by suppressing mTOR/SREBP-1/SCD1-mediated lipogenesis in PIK3CA-mutant colorectal cancer. Redox Biol. 2022;55:102426. https://doi.org/10.1016/j.redox.2022.102426.
19. Chen J, Zhao R, Wang Y, Xiao H, Lin W, Diao M, He S, Mei P, Liao Y. G protein-coupled estrogen receptor activates PI3K/AKT/mTOR signaling to suppress ferroptosis via SREBP1/SCD1-mediated lipogenesis. Mol Med. 2024;30(1):28. https://doi.org/10.1186/s10020-023-00763-x.
20. Ritter J, Bielack SS, Osteosarcoma. Ann Oncol 21 Suppl. 2010;7https://doi.org/10.1093/annonc/mdq276.
21. Kandasamy P, Gyimesi G, Kanai Y, Hediger MA. Amino acid transporters revisited: New views in health and disease. Trends Biochem Sci. 2018;43(10):752–89. https://doi.org/10.1016/j.tibs.2018.05.003.
22. Alam S, Doherty E, Ortega-Prieto P, Arizanova J, Fets L. Membrane transporters in cell physiology, cancer metabolism and drug response. Dis Model Mech. 2023;16(11). https://doi.org/10.1242/dmm.050404.
23. Pizzagalli MD, Bensimon A, Superti-Furga G. A guide to plasma membrane solute carrier proteins. FEBS J. 2021;288(9):2784–835. https://doi.org/10.1111/febs.15531.
24. He Y, Sun MM, Zhang GG, Yang J, Chen KS, Xu WW, Li B. Targeting PI3K/Akt signal transduction for cancer therapy. Signal Transduct Target Ther. 2021;6(1):425. https://doi.org/10.1038/s41392-021-00828-5.
25. Fresno Vara JA, Casado E, de Castro J, Cejas P, Belda-Iniesta C, Gonzalez-Baron M. PI3K/Akt signalling pathway and cancer. Cancer Treat Rev. 2004;30(2):193–204. https://doi.org/10.1016/j.ctrv.2003.07.007.
26. Wang C, Yang Z, Xu E, Shen X, Wang X, Li Z, Yu H, Chen K, Hu Q, Xia X, Liu S, Guan W. Apolipoprotein C-II induces EMT to promote gastric cancer peritoneal metastasis via PI3K/AKT/mTOR pathway. Clin Transl Med. 2021;11(8). https://doi.org/10.1002/ctm2.522.
27. Miricescu D, Totan A, Stanescu S, II SC, Badoiu C, Stefani M, Greabu. PI3K/AKT/mTOR Signaling Pathway in Breast Cancer: From Molecular Landscape to Clinical Aspects. Int J Mol Sci. 2020;22(1). https://doi.org/10.3390/ijms22010173.
28. Li H, Shen X, Ma M, Liu W, Yang W, Wang P, Cai Z, Mi R, Lu Y, Zhuang J, Jiang Y, Song Y, Wu Y, Shen H. ZIP10 drives osteosarcoma proliferation and chemoresistance through ITGA10-mediated activation of the PI3K/AKT pathway. J Exp Clin Cancer Res. 2021;40(1):340. https://doi.org/10.1186/s13046-021-02146-8.
29. Hensley CT, Wasti AT, DeBerardinis RJ. Glutamine and cancer: cell biology, physiology, and clinical opportunities. J Clin Invest. 2013;123(9):3678–84. https://doi.org/10.1172/JCI69600.
30. Altman BJ, Stine ZE, Dang CV. From Krebs to clinic: glutamine metabolism to cancer therapy. Nat Rev Cancer. 2016;16(10):619–34. https://doi.org/10.1038/nrc.2016.71.
31. Kodama M, Nakayama KI. A second Warburg-like effect in cancer metabolism: The metabolic shift of glutamine-derived nitrogen: A shift in glutamine-derived nitrogen metabolism from glutaminolysis to de novo nucleotide biosynthesis contributes to malignant evolution of cancer. BioEssays. 2020;42(12):e2000169. https://doi.org/10.1002/bies.202000169.
32. Yang L, Venneti S, Nagrath D. Glutaminolysis: A Hallmark of Cancer Metabolism. Annu Rev Biomed Eng. 2017;19:163–94. https://doi.org/10.1146/annurev-bioeng-071516-044546.
33. Cluntun AA, Lukey MJ, Cerione RA, Locasale JW. Glutamine Metabolism in Cancer: Understanding the Heterogeneity. Trends Cancer. 2017;3(3):169–80. https://doi.org/10.1016/j.trecan.2017.01.005.
34. Diaz-Vivancos P, de Simone A, Kiddle G, Foyer CH. Glutathione–linking cell proliferation to oxidative stress. Free Radic Biol Med. 2015;89:1154–64. https://doi.org/10.1016/j.freeradbiomed.2015.09.023.
35. Franco R, DeHaven WI, Sifre MI, Bortner CD, Cidlowski JA. Glutathione depletion and disruption of intracellular ionic homeostasis regulate lymphoid cell apoptosis. J Biol Chem. 2008;283(52):36071–87. https://doi.org/10.1074/jbc.M807061200.
36. Lee M, Cho T, Jantaratnotai N, Wang YT, McGeer E, McGeer PL. Depletion of GSH in glial cells induces neurotoxicity: relevance to aging and degenerative neurological diseases. FASEB J. 2010;24(7):2533–45. https://doi.org/10.1096/fj.09-149997.
37. Niu B, Liao K, Zhou Y, Wen T, Quan G, Pan X, Wu C. Application of glutathione depletion in cancer therapy: Enhanced ROS-based therapy, ferroptosis, and chemotherapy. Biomaterials. 2021;277:121110. https://doi.org/10.1016/j.biomaterials.2021.121110.
38. Dixon SJ, Olzmann JA. The cell biology of ferroptosis. Nat Rev Mol Cell Biol. 2024;25(6):424–42. https://doi.org/10.1038/s41580-024-00703-5.
39. Yi J, Zhu J, Wu J, Thompson CB, Jiang X. Oncogenic activation of PI3K-AKT-mTOR signaling suppresses ferroptosis via SREBP-mediated lipogenesis. Proc Natl Acad Sci U S A. 2020;117(49):31189–97. https://doi.org/10.1073/pnas.2017152117.

Publisher's note